

PAPER • OPEN ACCESS

Analysis of Handling Stability of Hydraulic Hybrid Vehicle based on ADAMS/Car Simulation

To cite this article: Chao Wang *et al* 2018 *IOP Conf. Ser.: Earth Environ. Sci.* **186** 012049

View the [article online](#) for updates and enhancements.



IOP | ebooks™

Bringing you innovative digital publishing with leading voices to create your essential collection of books in STEM research.

Start exploring the **collection** - download the first chapter of every title for free.

Analysis of Handling Stability of Hydraulic Hybrid Vehicle based on ADAMS/Car Simulation

Chao Wang¹, Xiaohui He¹, Xinmin Shen^{1,2,*}, Jingwei Zhu¹, Qin Yin¹, and Lei Xu¹

¹College of Field Engineering, Army Engineering University, No. 1 Haifu Street, Nanjing, Jiangsu, P. R. China

²Department of Industrial and Systems Engineering, The Hong Kong Polytechnic University, Hung Hom, Kowloon, Hong Kong SAR, P. R. China

Email: shenxmjflgdx2014@163.com

Abstract. Hydraulic hybrid vehicle is developed from the traditional vehicle by installation of the hydraulic system and disassembly of the mechanical transmission system, which influences the handling stability by changes of the centroid. Three layout schemes of the hydraulic system in hydraulic hybrid vehicle were proposed in this study, which were based on available space of the vehicle and size of the major hydraulic component. According to virtual prototype model of the vehicle constructed in ADAMS/Car software, simulations of the three layout schemes on steering angle step input test, steering angle pulse test and snake formation test were conducted. Scores of the steering angle step input test, steering angle pulse test and snake formation test of the T-type layout were 82, 80.72 and 93.42. Meanwhile, these of the postposition layout were 76, 79.46, and 91.11, and these of the parallel layout were 86, 82.19 and 95.55. Therefore, the final scores of these three layout schemes were 256.14, 246.57, and 263.74, respectively. Simulation results indicated that the parallel layout exhibited the best handling stability, which would be propitious to improve comprehensive performance of the hydraulic hybrid vehicle.

1. Introduction

Fuel economy and dynamic performance of the vehicle were important influence factors to evaluate its comprehensive property [1]. The classical vehicle takes the internal combustion engine as the power supply, and the power is transmitted by mechanical transmission system [2]. There exists an optimal workspace for the internal combustion engine, which can obtain a better fuel economy [3]. However, it cannot work in this optimal workspace most of time, because driving condition of the vehicle changes frequently [4]. Therefore, how to keep the internal combustion engine works in the optimal workspace is focus of research in the fields of vehicle kinematics and dynamics [5].

Hybrid vehicle is vehicle includes two or more power supplies, which has been developed with the aim of improvement of the fuel economy and dynamics performance [6]. It can take full advantage of each kinds of power supply and obtain their optimal match by the energy control strategy [7], which makes it a promising vehicle type [8]. Relative to other hybrid vehicle, hydraulic hybrid vehicle has the advantages of a strong power, easy controllability, low cost, and so on, which is considered as an ideal vehicle type for the large-scale construction machinery and special vehicle [9].

The studied hydraulic hybrid vehicle is developed from the traditional vehicle by installation of the hydraulic system and disassembly of the mechanical transmission system, which affects the handling stability by change of the centroid [10]. Virtual prototype model of the vehicle was constructed in the ADAMS/Car software, and three layout schemes of the hydraulic system in hydraulic hybrid vehicle



were proposed, which includes the T-type, postposition type, and parallel type. According to the test requirement of the handling stability in the national standard, steering angle step input test, steering angle pulse test, and snake formation test of the three schemes were conducted respectively, and each test was scored. Based on comprehensive scores of each scheme, the optimal layout can be concluded.

2. Layout scheme design

For the studied hydraulic hybrid vehicle, the available space includes three parts: below the back row seats (1460mm*1290mm*600mm), the trunk (1345mm*963mm*1400mm), and the original area for the gearbox (500mm*216mm*355mm), which is achieved by disassembly of mechanical transmission system. The hydraulic pump should connect the engine through the coupling, so it must be installed at the original area for the gearbox. Meanwhile, except the hydraulic pump and the accumulator, size and weight of the other hydraulic components are small, and their installations have few influences to the centroid. Therefore, installation of the accumulator is the major influence factor to handling stability. Size and weight of the accumulator are 1185mm*351mm*351mm and 140kg respectively, and those of the hydraulic pump are 477mm*200mm*349mm and 90kg respectively.

The T-type layout, postposition type layout, and the parallel type layout were shown in Figure 1. In the T-type layout in Figure 1(a), one hydraulic accumulator was installed in the central bottom of the vehicle, and the other one was installed into the trunk next to the back row seats. Meanwhile, for the postposition type layout, the two hydraulic accumulators were installed symmetrically in the trunk, as shown in Figure 1(b). For the parallel type layout in Figure 1(c), the two hydraulic accumulators were installed symmetrically in the area below the back row seats.

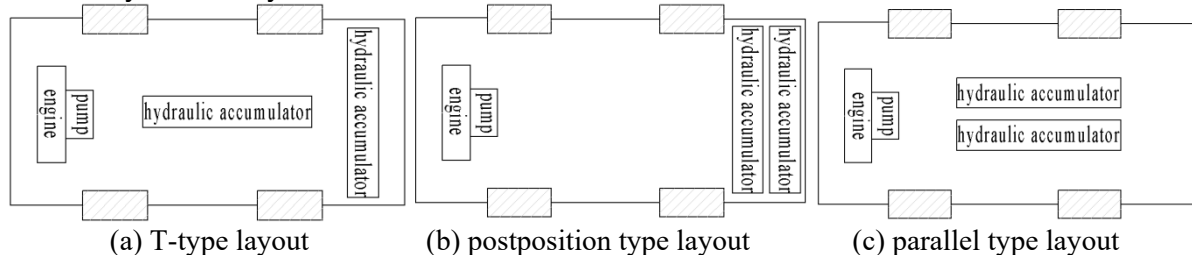


Figure 1. Schematic diagram of the three layout schemes of the hydraulic system.

3. Modeling and simulation

Virtual prototype model of the vehicle was constructed in the ADAMS/Car software, which includes body system, power system, transmission assembly system, front suspension system, steering system, back suspension system, tire system, and so on, as shown in Figure 2. Each system was modeled in the standard mode and constructed by existing subsystem module, and their parameters could be modified by the actual data. Critical parameters of the vehicle were summarized in Table 1.

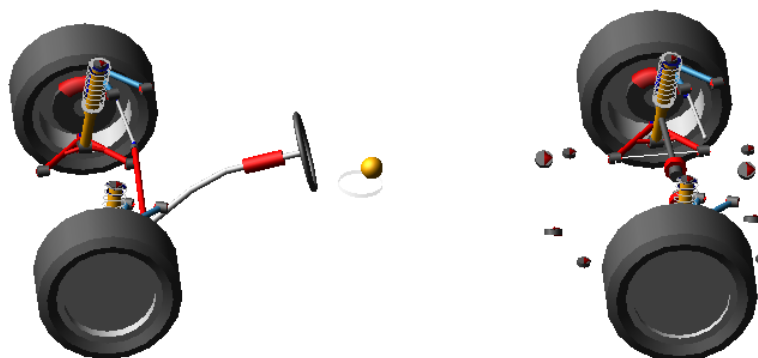


Figure 2. Virtual prototype model of the vehicle constructed in the ADAMS/Car software.

Table 1. Critical parameters of the studied hydraulic hybrid vehicle

Parameters	Values
Weight of the whole vehicle	2350kg
Front track	1540mm
Spring stiffness of front suspension	12.5N/mm
Caster angle of the kingpin	10°
Anterior beam angle	0.2°
Wheelbase	2800mm
Back track	1540mm
Spring stiffness of back suspension	12.5N/mm
Inclination angle of the kingpin	2.5°
Camber angle of the wheel	-0.5°

Simulation of the handling stability was conducted based on the GB/T6323 [11]. The steering angle step input test [12], steering angle pulse test [13], and snake formation test [14] of the three schemes were conducted respectively in the virtual prototype model.

3.1 Steering angle step input test

The steering angle step input test is analysis of the transient response of the whole vehicle, and its evaluation indexes include steady state value, response time, peak response time, and the maximum response value of the yaw rate. Among these evaluation indexes, response time of the yaw rate is the major one. Therefore, the steering angle step input test was conducted as shown in the Figure 3(a). The vehicle was going straight with speed 60km/h. At time of 3s, a step input of 0.3s was given to drive the steering wheel angle to 100°. Afterwards, the steering wheel was kept steady and the speed was kept constant. The corresponding evolution of response time of yaw rate was shown in Figure 3(b).

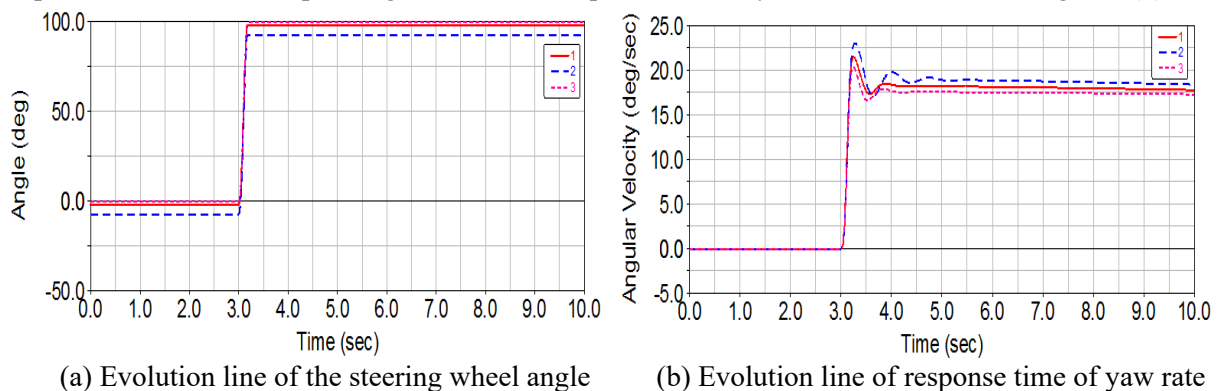


Figure 3. The steering angle step input test of the three schemes.

From the Figure 3(b) it could be calculated that the response time of yaw rate of the T-type layout, postposition type layout, and the parallel type layout were 0.19s, 0.22s, and 0.17s, respectively. For the purpose of scientific evaluation of score of each scheme, data of the response time was normalized based on the national standard GB/T13047-91, and the normalization was realized by Eq. 1.

$$N_i = 60 + \frac{40}{T_{60} - T_{100}} (T_{60} - T_i) \quad i = 1, 2, 3 \quad (1)$$

Here N_i is the normalized score of each scheme; T_{60} is the lower limit value of response time of yaw rate, 0.30s, which is fixed by the GB/T13047-91 [11]; T_{100} is the upper limit value of response time of yaw rate, 0.10s, which is also fixed by the GB/T13047-91; T_i is the response time of yaw rate of each scheme. Therefore, the normalized scores of T-type layout, postposition type layout, and the parallel type layout were 82, 76, and 86, respectively.

3.2 Steering angle pulse test

The steering angle pulse test was conducted by frequency response characteristics of the yaw rate, and the evaluation indexes include the resonant frequency, resonance peak level, and phase lag angle. Therefore, the steering angle pulse test was conducted as shown in Figure 4(a). The vehicle was going straight with speed of 60km/h. Afterwards, a pulse input with width of 0.5s was given to the steering wheel for maximum angle of 140°. The corresponding yaw rate was shown in Figure 3(b).

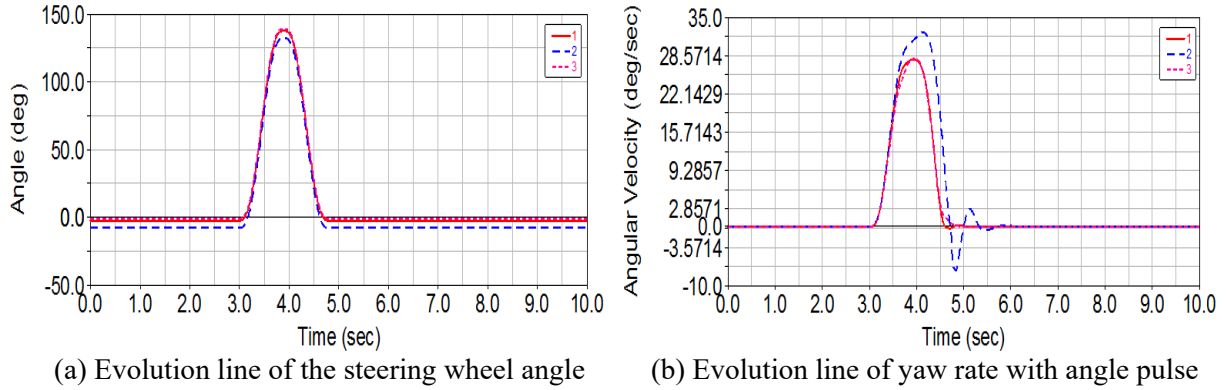


Figure 4. The steering angle pulse test of the three schemes.

Frequency response characteristics of the yaw rate $G(jkw_0)$ can be calculated by the Eq. 2. Here $r(t)$ is the yaw rate; $\theta(t)$ is the steering wheel angle; w_0 is the calculation interval of the frequency, 0.1Hz. According to the national standard GB/T13047-91, the obtained resonant frequency, resonance peak level, and the phase lag angle of the T-type layout were 0.62Hz, 3.28dB, and 26.10°, respectively. Meanwhile, those of the postposition type layout were 0.65Hz, 3.36dB, and 26.81°, and those of the parallel type layout were 0.58Hz, 3.21dB, and 25.30°.

$$G(jkw_0) = \frac{\int_0^r r(t) \cos kw_0 t dt - \int_0^r r(t) \sin kw_0 t dt}{\int_0^r \theta(t) \cos kw_0 t dt - \int_0^r \theta(t) \sin kw_0 t dt} \quad (2)$$

In order to scientifically evaluate the score of each scheme, data of the resonant frequency, resonance peak level, and the phase lag angle was normalized, and the applied equations were shown in Eq. 3, Eq. 4, and Eq. 5. Here N_{fi} is the normalized score of each scheme for the resonant frequency; f_{60} is the lower limit value of the resonant frequency, 0.7Hz; f_{100} is the upper limit value of resonant frequency, 1.30Hz; f_i is the resonant frequency of each scheme; N_{Di} is the normalized score of each scheme for the resonance peak level; D_{60} is the lower limit value of the resonance peak level, 5.00dB; D_{100} is the upper limit value of the resonance peak level, 2.00dB; D_i is the resonance peak level of each scheme; N_{ai} is the normalized score of each scheme for the phase lag angle; α_{60} is the lower limit value of the phase lag angle, 60°; α_{100} is the upper limit value of the phase lag angle, 20°; α_i is the phase lag angle of each scheme. The final score N_w of each scheme for the steering angle pulse test could be calculated by the Eq. 6, which was average of the N_f , N_D , and N_a , and it was 80.72, 79.46, and 82.19 for the T-type layout, postposition type layout, and parallel type layout, respectively.

$$N_{fi} = 60 + \frac{40}{f_{60} - f_{100}} (f_i - f_{60}) \quad (3)$$

$$N_{Di} = 60 + \frac{40}{D_{60} - D_{100}} (D_{60} - D_i) \quad (4)$$

$$N_{ai} = 60 + \frac{40}{\alpha_{60} - \alpha_{100}} (\alpha_{60} - \alpha_i) \quad (5)$$

$$N_{\omega} = \frac{N_f + N_D + N_{\alpha}}{3} \quad (6)$$

3.3 Snake formation test

The snake formation test is used to evaluate the steady state performance of the vehicle in condition of the continuous steering, which is suitable for the comprehensive evaluations of driving stability and ride comfort. The major evaluation indexes are the peak value of yaw rate and average steering wheel peak angle. Thus, the snake formation test was conducted by driving the vehicle with snake formation at the speed of 65km/h, and the simulation results were shown in Figure 5.

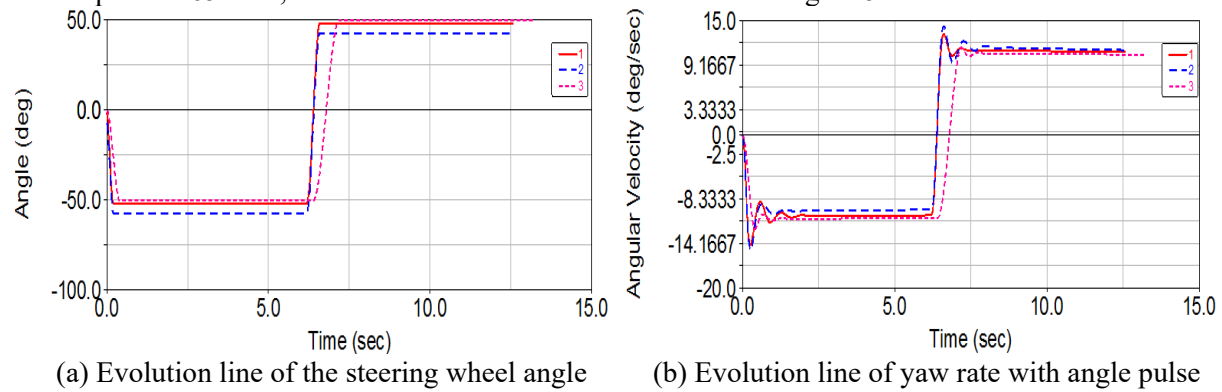


Figure 5. The snake formation test of the three schemes.

The peak value of yaw rate and average steering wheel peak angle of T-type layout were 13.7deg/s and 50°, respectively. Meanwhile, those of the postposition type layout were 15.0deg/s and 50°, and those of the parallel type layout were 12.5deg/s and 50°. Data of the two indexes were normalized by Eq. 7 and Eq. 8. Here N_{γ_i} and N_{θ_i} are the normalized score of each scheme for the peak value of yaw rate and average steering wheel peak angle; γ_i and θ_i are the peak value of yaw rate and the average steering wheel peak angle of each scheme; γ_{60} , γ_{100} , θ_{60} , and θ_{100} are 25deg/s, 10deg/s, 180°, and 60°, which are fixed by the QC/T480-1999 [15]. The final score N_s of each scheme for snake formation test average of the N_{γ} and N_{θ} . Therefore, the final scores of snake formation test for the T-type layout, postposition type layout, and the parallel type layout were 93.4, 91.1, and 95.5, respectively.

$$N_{\gamma_i} = 60 + \frac{40}{\gamma_{60} - \gamma_{100}} (\gamma_{60} - \gamma_i) \quad (7)$$

$$N_{\theta_i} = 60 + \frac{40}{\theta_{60} - \theta_{100}} (\theta_{60} - \theta_i) \quad (8)$$

Summarized simulation results were shown in Table. 2 and it could be found that the parallel type layout exhibited the best handling stability.

Table 2. Summarized simulation results of the three layout schemes

Layout schemes	T-type layout	Postposition type layout	Parallel type layout
Steering angle step input test	82.00	76.00	86.00

Steering angle pulse test	80.72	79.46	82.19
Snake formation test	93.42	91.11	95.55
Total	256.14	246.57	263.74

4. Conclusions

Handling stability of hydraulic hybrid vehicle for T-type layout, postposition type layout, and parallel type layout was analyzed based on ADAMS/Car simulation. The following conclusions were obtained.

(1) Virtual prototype model of the vehicle was constructed in the ADAMS/Car software, and three layout schemes of the hydraulic system in hydraulic hybrid vehicle were proposed.

(2) The steering angle step input test, steering angle pulse test, and snake formation test of the three schemes were conducted respectively, and the final scores of these three layout schemes were 256.14, 246.57, and 263.74, which indicated that the parallel type layout exhibited the best handling stability.

Acknowledgments

This work was supported by a grant from National Natural Science Foundation of China (51505498), a grant from Natural Science Foundation of Jiangsu Province (BK20150714), and a grant from National Key Research and Development Program of China (2016YFC0802900). Xinmin Shen was grateful for support from the Hong Kong Scholars Program (No. XJ2017025).

References

- [1] Sundström O, Guzzella L, Soltic P 2008 Optimal Hybridization in Two Parallel Hybrid Electric Vehicles using Dynamic Programming *IFAC Proceedings Volumes* **41(2)** 4642-4647
- [2] Yang W W, Liang J J Y, Yang J, Zhang N 2018 Investigation of a Novel Coaxial Power-Split Hybrid Powertrain for Mining Trucks *Energies* **11(1)** 172
- [3] Lucente G, Montanari M, Rossi C 2007 Modelling of an automated manual transmission system *Mechatronics* **17(2-3)** 73-91
- [4] Alagumalai A 2014 Internal combustion engines: Progress and prospects *Renewable and Sustainable Energy Reviews* **38(2014)** 561-571
- [5] Xu L L, Shen X M, Liu Q, Zhou J Z, Peng K 2017 Investigation on obstacle-surmounting capacity of biped-wheel unmanned platform based on kinematic and kinetic analysis *Procedia Engineering* **174(2017)** 219-226
- [6] Wang C, He X H, Shen X M, Yang X C, Xu L, Wang Q, Liu A X 2017 Optimal Design of Experimental Platform for Electronic-Hydraulic Driving Vehicle Based on the Multi-factor Synthetic Evaluation Model *Advances in Mechanical Design* **55(2018)** 271-283
- [7] Severin C, Pischinger S, Ogrzewall J 2005 Compact gasoline fuel processor for passenger vehicle APU *Journal of Power Sources* **145(2)** 675-682
- [8] Xu L, He X H, Shen X M, Yang X C, Wang C, Wang Q, Liu A X 2017 Investigation on the Optimal Energy Recovery System for the Military Hybrid Vehicle Based upon the Comprehensive Evaluation Method *Advances in Mechanical Design* **55(2018)** 923-935
- [9] Sun H, Jiang J H, Wang X 2009 Torque control strategy for a parallel hydraulic hybrid vehicle *Journal of Terramechanics* **46(6)** 259-265
- [10] Sun H, Yang L F, Jing J Q 2010 Hydraulic/electric synergy system (HESS) design for heavy hybrid vehicles *Energy* **35(12)** 5328-5335
- [11] Wu B G, Yan S F, Li S P, Tian M J 2014 Vehicle Handling Stability Simulation *Machinery Design & Manufacture* **11** 158-160
- [12] Wang H, Yang L, Feng Y, Peng R J 2014 Simulation of Modeling and Handling Stability of a Racing Vehicle Based on ADAMS *Journal of Guangdong University of Technology* **31(2)** 104-108
- [13] Hu L, Fang S Y, Yang J 2014 Study of the Vehicle Controllability and Stability Based on Multi-body System Dynamics *The Open Mechanical Engineering Journal* **8** 865-871
- [14] Wang S, Yu Q, Zhao X 2018 Study on driver's turning intention recognition hybrid model of

- GHMM and GGAP-RBF neural network *Advances in Mechanical Engineering* **10(3)** 1-16
- [15] Zang H, Yu Z, Xiong L 2016 The Influences of the Subframe Flexibility on Handling and Stability Simulation When Using ADAMS/Car *SAE International Journal of Passenger Cars - Mechanical Systems* **9(2)** 861-868